

Relational dynamic memory networks

Trang Pham, Truyen Tran and Svetha Venkatesh
 Applied AI Institute, Deakin University, Australia
{phtra, truyen.tran, svetha.venkatesh}@deakin.edu.au

Abstract

Working memory is an essential component of reasoning – the capacity to answer a new question by manipulating acquired knowledge. Current memory-augmented neural networks offer a differentiable method to realize limited reasoning with support of a working memory module. Memory modules are often implemented as a set of memory slots without explicit relational exchange of content. This does not naturally match multi-relational domains in which data is structured. We design a new model dubbed Relational Dynamic Memory Network (RDMN) to fill this gap. The memory can have a single or multiple components, each of which realizes a multi-relational graph of memory slots. The memory is dynamically updated in the reasoning process controlled by the central controller. We evaluate the capability of RDMN on several important application domains: software vulnerability, molecular bioactivity and chemical reaction. Results demonstrate the efficacy of the proposed model.

Keywords: Memory-augmented neural networks; graph neural networks; relational memory; graph-graph interaction

1 Introduction

Reasoning is the process of forming answer to a new question by manipulating previously acquired knowledge [8]. This capacity necessitates a working memory to load, hold, integrate and alter information [16]. A recent fruitful research direction for solving this problem is by augmenting a neural network with a differentiable “working memory” module to account for long-term dependencies in computing the answer [24, 37, 62]. The memory enables temporary storing of partial findings, which can then be iteratively refined to produce the final answer. The entire system can be trained end-to-end in a “differentiable programming” fashion. Technically, memory provides a short-cut for passing signal and gradient between query, input and output [40], akin to a popular technique known as skip-connection [25, 27, 48, 60]. This makes credit-assignment easier in a long chain of computation. These “working memory” modules have been developed to be generic without considering the structural information that may be available in the object being queried. A typical memory module is a fixed set of memory cells. For structured objects such as graphs, encoding structural information into memory is not straightforward [24]. We conjecture that a memory structure that is reflective of the structure of the data might be easier to train and generate a more focused answer.

To that end, we propose a neural architecture called Relational Dynamic Memory Networks (RDMN) [50] to answer queries about structured data¹. We consider the case where data is structured as attributed graphs, e.g., molecular graphs or function call graphs in software. RDMN is composed of a controller and *a structured dynamic memory organized as a network of cells*, inspired by the current understanding of working memory as a dynamic network [9, 20, 61]. The controller handles the I/O processes and updates the memory. The memory graph is dynamically defined by the structure within the input data conditioned on the query. The memory cells interact with each other during the reasoning process, and the memory content is refined along the way. In particular, the state of a memory cell is updated by aggregating the write content from the controller as well as the messages sent by neighbor cells. Memory can have a single component or multiple interacting components. In this paper, we limit ourselves to the case where the memory network is structurally reflective of the input graphs. In particular, each memory cell maintains the state of an input node throughout the reasoning process.

The RDMN permits answering queries about not just a single graph, but also several graphs. An example of single graph is predicting whether a drug molecule (a graph) has any positive effect on a type of disease (a query). In this setting, raw atom descriptors (or atom embedding) are loaded into memory cells, one atom per cell, and chemical bonds dictate cell connections. The query is embedded to a vector, which is read by the controller, whose operations guide the evolution of the memory states toward the answer (e.g., yes or no). Another example is in software, and this is manifested through intra-module function calls in software. Here each software module is a graph of function call, and the query can be anything about the result of execution of the module.

Querying over several graphs can be cast as modeling of *graph-graph interaction*, which is an under-explored problem in its own right. The interaction may range from graph similarity (e.g., graph kernels as in [64]) to more complex settings. An example is to ask whether two molecules (graphs) engage in a particular chemical reaction setting (a query) [21, 38]. In the example of software, this is manifested through inter-module interactions to solve a given problem (a query). The RDMN supports graph-graph interaction through the reasoning over multi-component memory.

In summary, we claim the following contributions:

- A novel differentiable structured working memory module augmented to a neural network dubbed Relational Dynamic Memory Networks (RDMN).
- A general solution for answering queries about one or more graphs. In particular, it solves a relatively novel problem of predicting graph-graph interaction.
- A validation of RDMN three distinct tasks: software source code vulnerability assessment, molecular bioactivity prediction, and chemical reaction prediction.

The rest of the paper is organized as follows. Section 2 reviews related work, followed by preliminaries on memory-augmented neural networks and graph neural networks in Section 3. The main contribution of the paper, the RDMN, is described in Section 4 with implementation detailed in Section 5. Experiments and results are reported in Section 6. Section 7 discusses implications and concludes the paper.

¹A preliminary version of this work was published in a conference [50].

2 Related work

Working memory and reasoning

This paper is partly inspired by the concept of “working memory”, a brain faculty for holding and manipulating information for an extended period of time [4]. Working memory is a critical component that enables high-level cognition (e.g., reasoning, meta-reasoning) [16]. Observations found that working memory arises through functional coordination between brain regions [61], which may suggest the graph-theoretical approach for cognitive modeling. Some studies focus on the maintenance of neural activities over an extended period of time (e.g., seconds or more), but other work suggests the fast modification of synapses to play a key role [20, 44]. An important feature of working memory is the fast loading (or binding) of information into the memory, allowing rapid task-switching and selective attention [7]. Our work draws inspiration from these findings and theory, but does not aim to be biologically relevant.

Rather we aim for building a neural network capable of *neural reasoning* [24, 31]. This capability is needed for tasks such as graph traversal [24], knowledge graph completion [58], textual QA [66] and visual QA [1, 47]. To facilitate relational reasoning, recent neural networks [30, 55] have been proposed to model pair-wise relationship between objects. A recurrent variant allows more dynamic reasoning process [54]. Our work contributes to this line of research by introducing a controller into a relational memory module, and thus helping in answering arbitrary queries.

Graph representation and querying

There has been a surge of interest in learning graph representation for the past few years [10, 11, 28, 33, 41, 42, 45, 57, 67, 68]. A number of works derive shallow unsupervised embedding methods such as node2vec and subgraph2vec, possibly inspired by the success of embedding in linear-chain text (word2vec and paragraph2vec). Deep spectral methods have been introduced for graphs of a given adjacency matrix [11], whereas we allow arbitrary graph structures, one per graph. Several other methods extend convolutional operations to irregular local neighborhoods [3, 45, 49], or employ recurrent paths along the random walk from a node [56]. Graph dynamics has been recently studied. Gated Graph Transformer [33] allows dynamics over time with graph state transition. Finally, there is a growing body of generative models of graphs which aim to either model the entire distribution of graphs or to generate realistic graphs (e.g., see [42, 68] and references therein).

Related to but distinct from our work is the work about querying on graphs in the database community [43]. There are sub-problems that can benefit from RDMN, however, including graph matching, maximum clique and segmentation (clustering). Our work adds to the existing literature by allowing arbitrary querying from a single or multiple graphs. Note that our querying system allows answering with inferred knowledge instead of just factual knowledge.

Memory-augmented neural nets (MANN)

MANN is a recent development in deep learning where the goal is to add an external memory model to a processor. This arises from the realization that many realistic tasks

involve a long series of computation, and current RNNs are ineffective. A differentiable memory module would allow greater storage and efficient recall of intermediate results. Notable architectures include Neural Turing Machine [23] and its recent cousin, the Differentiable Neural Computer [24]. Here all operations are differentiable, and the memory is dynamically updated along the I/O and reasoning steps. This design is powerful but poses great challenges for implementation. End-to-End Memory Networks [62] simplify this by loading the entire input matrix into the memory and fixing the memory content. Similar architectures have been subsequently proposed to solve specific tasks, including the Dynamic Memory Networks for question-answering problems [37], the Recurrent Entity Net [29] for tracking entities, and the key-value structure for rare-events [34].

Limited work has been done for the structured memory [6, 46, 54]. Our RDMN differs from these models by using a dynamic memory organized as a graph of cells. The cells interact not only with the controller but also with other cells to embed the substructure in their states. A potential mechanism for a dynamic working memory is introduced in [18, 54], where memory dynamics can be modeled as recurrent matrices. Relations between cells are either learned [18] or dynamically estimated through self-attention [54]. Our work builds on top of this memory module by introducing a controller to manage update of the memory matrix.

MANN has found a wide range of applications, including question-answering [37, 62], graph processing [24], algorithmic tasks [24], meta-learning [53], healthcare [40] and dialog systems [39]. Our work introduces a new set of applications in biochemistry and software.

Software and molecular graphs

Our application of RDMN for software is in line with the current direction of modeling source code using structures such as trees [14] and graphs [2]. The recurrent nature of the RDMN, in principle, would capture a program execution without actually running the code [12].

Our application to chemical compound classification bears some similarity to the work of [19], where graph embedding is also collected from node embedding at each layer and refined iteratively from the bottom to the top layers. However, our treatment is more principled and more widely applicable to multi-typed edges. An application of neural networks for molecular activity prediction is to train a neural network on an assay toward a specific test. This method can fit and predict the data well when the training data is sufficient. However, molecular activity tests are costly, hence, the datasets are normally small, causing overfitting on neural network models. To improve the prediction performance, multiple tests can be jointly trained by a single neural network. The model for multi-task learning is still a neural network that reads the input feature vector, but there is a separated output for each task. This model has been applied successful in work for molecular activity prediction such as QSAR prediction [13, 17], massive drug discovery [51] with a large dataset of 40M measurements over more than 200 tests and toxicity prediction challenge [63].

In predicting chemical reactions, there has been limited work leveraging deep neural networks [21, 32, 38]. We contributes to the literature by introducing a generic Turing machine-like architecture that can answer arbitrary queries about interaction between chemical compounds.

3 Preliminaries

3.1 Memory-augmented neural nets

Following the setting of Neural Turing Machine [23], a MANN consists of an external memory and a controller, both evolving over time. At each time step, the controller reads an input, updates the memory, and emits an output. Memory is often modeled as a matrix whose columns are memory slots. With stationary update rules, the memory can be rolled out over time into a recurrent matrix net [18]. Let us denote the activation memory matrix as $\mathbf{M} \in \mathbb{R}^{d \times m}$ for d dims and m slots. Upon seeing new evidence \mathbf{x} (which could be empty), the controller generates a write vector $\mathbf{w} \in \mathbb{R}^p$ which causes a candidate memory update:

$$\tilde{\mathbf{M}} \leftarrow \phi(W\mathbf{w}\mathbf{1}^\top + U\mathbf{M}\mathbf{R} + B) \quad (1)$$

where $W \in \mathbb{R}^{d \times p}$ is data encoding matrix, $U \in \mathbb{R}^{d \times d}$ is transition matrix, $\mathbf{R} \in \mathbb{R}^{m \times m}$ is the graph of relation between memory slots, and $B \in \mathbb{R}^{d \times m}$ is bias. Memory is then updated as: $\mathbf{M} \leftarrow f(\mathbf{M}, \tilde{\mathbf{M}})$ for some function f . For example, a skip-connection in $f(\mathbf{M}, \tilde{\mathbf{M}}) = \alpha * \mathbf{M} + (1 - \alpha) * \tilde{\mathbf{M}}$, where $*$ is element-wise multiplication, and $\alpha \in (0, 1)$ is learnable forget-gate.

Often, the controller must read the memory to determine what to do next. For example, the End-to-End Memory Network [62] maintains a dynamic state of an answer \mathbf{u} by reading the memory as follows:

$$\begin{aligned} \mathbf{a} &\leftarrow \text{softmax}(\mathbf{M}^\top (\mathbf{A}\mathbf{u})) \\ \mathbf{u} &\leftarrow \mathbf{U}\mathbf{u} + \mathbf{C}\mathbf{M}\mathbf{a} \end{aligned}$$

where $\mathbf{A}, \mathbf{U}, \mathbf{C}$ are trainable parameters. Here $\mathbf{k} = \mathbf{A}\mathbf{u}$ plays the role of a key in the content-addressing scheme, and \mathbf{a} assigns an attention weight to each memory slot.

3.2 Graph neural networks

A graph is a tuple $\mathbf{G} = \{\mathbf{A}, \mathbf{R}, \mathbf{X}\}$, where $\mathbf{A} = \{a^1, \dots, a^M\}$ are M nodes. $\mathbf{X} = \{\mathbf{x}^1, \dots, \mathbf{x}^M\}$ is the set of node features, where \mathbf{x}^i is the feature vector of node a^i . \mathbf{R} is the set of relations in the graph. Each tuple $\{a^i, a^j, r, \mathbf{b}^{ij}\} \in \mathbf{R}$ describes a relation of type r ($r = 1 \dots R$) between two nodes a^i and a^j . The relations can be one-directional or bi-directional. The vector \mathbf{b}^{ij} represents the link features. Node a^j is a neighbor of a^i if there is a connection between the two nodes. Let $\mathcal{N}(i)$ be the set of all neighbors of a^i and $\mathcal{N}_r(i)$ be the set of neighbors connected to a^i through type r . This implies $\mathcal{N}(i) = \cup_r \mathcal{N}_r(i)$.

Graph neural networks are a class of neural nets that model the graph structure directly. The most common type is message passing graph neural networks [22, 49, 56], which update node states using messages sent from the neighborhood. In the *message aggregation* step, we combine multiple messages sent to node i into a single message vector \mathbf{m}_i :

$$\mathbf{m}_i^t = g^a \left(\mathbf{x}_i^{t-1}, \left\{ (\mathbf{x}_j^{t-1}, \mathbf{e}_{ij}) \right\}_{j \in \mathcal{N}(i)} \right) \quad (2)$$

where $g^a(\cdot)$ can be an attention [5] or a pooling architecture. During the *state update* step, the node state is updated as follows:

$$\mathbf{x}_i^t \leftarrow g^u(\mathbf{x}_i^{t-1}, \mathbf{m}_i^t) \quad (3)$$

where $g^u(\cdot)$ can be any type of deep neural networks such as MLP [35], RNN [56], GRU [41] or Highway Net [49].

4 Relational dynamic memory

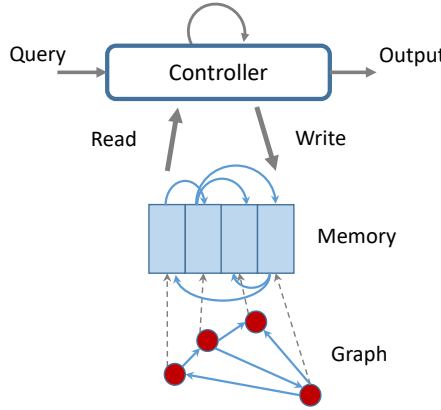


Figure 1: RDMN with single component memory. At the first step, the controller reads the query; the memory is initialized by the input graph, one node embedding per memory cell. Then during the reasoning process, the controller iteratively reads from and writes to the memory. Finally, the controller emits the output.

In this section, we present our main contribution, the Relational Dynamic Memory Network (RDMN), which is built upon two separate concepts, the Memory-Augmented Neural Net (see Section 3.1) and Graph Neural Net (see Section 3.2). RDMN can have a single-component memory as illustrated in Fig. 1 or multi-component memory as illustrated in Fig. 2.

Let us start with the RDMN that consists of a controller and a single-component memory module. The system, when rolled out during reasoning, is two recurrent neural networks (RNNs) interacting with each other. Different from the standard RNNs, the memory is a matrix RNN [18], where the hidden states are matrices with a graph imposed on cells. The controller first takes the query as the input and repeatedly reads from the memory, processes and sends the signals back to the memory cells. Then at each reasoning step, the cell content is updated by the signals from the controller and its neighbor memory cells in the previous step. Through multiple steps of reasoning, the memory cells are evolved from the original input to a refined stage, preparing the controller for generating the output.

4.1 Encoder

The I/O processes prepare data for the reasoning process, i.e., encoding queries into the controller and data into the memory. Let q be the query, which is encoded into a vector as:

$$\mathbf{q} = \text{q_encode}(q) \quad (4)$$

Examples of query include a prediction task, a question or a retrieval cue.

Let X be the information context, which can be either input data (e.g., available directly, or as an output of a sensing module), or information retrieved from episodic memory (e.g., as response to the retrieval cue q). X is then loaded into the memory module \mathbf{M} consisting of K memory cells:

$$\mathbf{M} = \text{m_load}(X, q) \quad (5)$$

Assume that the query and context together impose a set \mathcal{R} of pairwise relations between memory cells. More precisely, any pair of cells will have zero or more relations drawn from the relation set. For example, if X is a molecule, and q is a bioactivity, then $\mathbf{M}[i]$ can be the embedding of the atom at node i of the molecular graph, and the relations can be bonding types (e.g., ion or valence bonds). Another example is in computer vision where X is an image, $\mathbf{M}[i]$ is an object embedding through a CNN for object detection, and the relations are the interaction types between objects (e.g., man-ride-horse). The relations can be modeled as a collection of adjacency matrices² $\mathbf{A} = \{A_r\}_{r \in \mathcal{R}}$.

Given q and \mathbf{M} , the controller computes the output probability $P_\theta(\mathbf{y} | \mathbf{M}, q)$. In what follows, we present how the computation occurs.

4.2 Reasoning processes

The controller manages the reasoning process by updating its own state and the working memory. Let \mathbf{h}_t be the state of the controller at time t ($t = 0, \dots, T$). At time $t = 0$, the state is initialized as $\mathbf{h}_0 = q$. During the multi-hop reasoning process to answer the query, the controller retrieves a content \mathbf{r}_t from the memory at time t and updates its state and memory as follows:

$$\mathbf{r}_t = \text{m_read}(\mathbf{M}_{t-1}, \mathbf{h}_{t-1}) \quad (6)$$

$$\mathbf{h}_t = \text{s_update}(\mathbf{h}_{t-1}, \mathbf{r}_t) \quad (7)$$

$$\mathbf{M}_t = \text{m_update}(\mathbf{M}_{t-1}, \mathbf{h}_t, \mathbf{A}) \quad (8)$$

The read operator can have multiple read heads, and the output is aggregated (e.g., averaged).

4.3 Decoder

At the end of the reasoning process, the controller predicts an output, that is

$$\mathbf{y} = \text{decode}(\mathbf{h}_T, q) \quad (9)$$

The decoder is a task-specific model, which could be a deep feedforward net for vector output, or a RNN for sequence output.

²For now we assume the adjacent matrices are given for a problem, but they could be learned dynamically, e.g., see the recent work in [67].

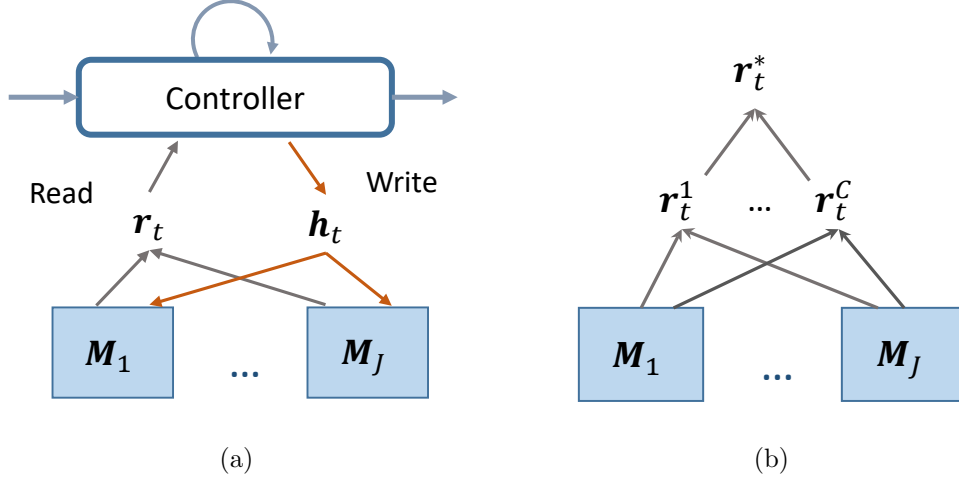


Figure 2: (a) RDMN with multi-component memory. (b) Multiple attention read heads

4.4 Multi-component memory

We now extend the single-component RDMN into multi-components³. Here each component is a multi-relational memory itself with the adjacent matrices \mathbf{A}_c and relation set \mathcal{R}_c . Examples include chemical reaction between multiple molecules, each of which can be loaded into a relational memory component. The central controller handles the interaction between the components. With iterative estimation, the controller can repeatedly refine the interaction representation before producing a prediction.

$$\mathbf{r}_t^* = \text{r_aggregate} \{ \mathbf{r}_{tc} \}_{c=1}^C \quad (10)$$

Eqs. (6,8) are component-specific but share controller state \mathbf{h}_t and Eq. (7) remains unchanged. See Fig. 2 for an illustration.

5 An implementation

We now present a specific realization of the generic framework proposed in Section 4 and validated in Section 6. All operators are parameterized and differentiable. This supports efficient gradient-based end-to-end learning⁴.

- For the **m_read** operator in Eq. (6), a content-based addressing scheme, also known as soft attention, is employed. At each time step t ($t = 1, \dots, T$), \mathbf{r}_t is a sum of all memory cells, weighted by the attention probability a_t^i , for each memory cell

³It is possible to generalize to multiple controllers with shared multiple memories, e.g., see [40].

⁴Discrete operators can also be implemented with help of reinforcement learning algorithms such as REINFORCE [65].

$i = 1, \dots, K$:

$$\begin{aligned}\mathbf{a}_t &= \text{attention}(\mathbf{M}_t, \mathbf{h}_{t-1}) \\ \mathbf{r}_t &= \mathbf{M}_t \mathbf{a}_t\end{aligned}$$

where attention is implemented as follows:

$$a_t^i = \text{softmax}(\mathbf{v}^\top \tanh(W_a \mathbf{M}_{t-1}[i] + U_a \mathbf{h}_{t-1})). \quad (11)$$

- The controller can be implemented in several ways. It could be a feedforward network or a recurrent network such as LSTM/GRU. In case of feedforward net, the query information is propagated through the memory via memory update. In case of recurrent nets, the query information is also propagated through the internal state of the controller. Here we use the RNN update style, where **s_update** operator in Eq. (7) reads:

$$\tilde{\mathbf{h}}_t = g(W_h \mathbf{h}_{t-1} + U_h \mathbf{r}_t) \quad (12)$$

- For the **m_update** operator in Eq. (8), the memory is updated as follows:

$$\tilde{\mathbf{M}}_t = g\left(U_m \mathbf{h}_t \mathbf{1}^\top + W_m \mathbf{M}_{t-1} + \sum_r V_r \mathbf{M} \hat{A}_r\right) \quad (13)$$

where \hat{A}_r is the normalized adjacency matrix, that is, $\hat{A}_r[i, j] = \frac{A_r[i, j]}{\sum_i A_r[i, j]}$. This is similar to Eq. (1).

- The **r_aggregate** operator in Eq. (10) is simply an averaging, i.e.,

$$\mathbf{r}_t^* = \frac{1}{C} \sum_{c=1}^C \mathbf{r}_{tc}$$

The attention mechanism in Eq. (11) can be overly restricted. This can be extended straightforwardly to multiple read-heads to produce multiple read vectors $\{\mathbf{r}_t^1, \mathbf{r}_t^2, \dots, \mathbf{r}_t^F\}$. This is followed by some pooling operator, e.g., mean pooling: $\mathbf{r}_t = \frac{1}{F} \sum_f \mathbf{r}_t^f$. Alternatively, the **s_update** operators in Eq. (12) can be modified to handle multiple read vectors, e.g., $\mathbf{h}_t = g\left(W_h \mathbf{h}_{t-1} + \sum_f U_h^f \mathbf{r}_t^f\right)$.

5.1 Recurrent skip-connections

Skip-connections are known to ease training [27, 60]. Here we implement both the controller and the memory updates using the following [48, 60]:

$$\mathbf{z}_t = \boldsymbol{\alpha} * \mathbf{z}_{t-1} + (1 - \boldsymbol{\alpha}) * \tilde{\mathbf{z}}_t$$

where $*$ is element-wise multiplication, $\boldsymbol{\alpha}$ is a sigmoid gate moderating the amount of information flowing from the previous step, \mathbf{z}_{t-1} is the state from the previous step and $\tilde{\mathbf{z}}_t$ is a proposal of the new state which is typically implemented as a nonlinear function of \mathbf{z}_{t-1} .

The controller \mathbf{h}_t and the memory cells $\mathbf{M}_t[i]$ are updated in a fashion similar to that of \mathbf{z}_t while $\tilde{\mathbf{h}}_t$ and $\tilde{\mathbf{M}}_t[i]$ are computed as in Eqs. (12,13). This makes the memory cell update similar to that of Differentiable Neural Computer [24], where the memory cells are partially erased and updated with new information.

Remark: With this choice, the entire network can be considered as $M + 1$ RNNs interacting following the structure defined by the multi-relational graph.

5.2 RDMN for multi-task learning

RDMN can be easily applied for multi-task learning. Suppose that the dataset contains n tasks. We can use the query to indicate the task. If a graph is from task k , the query for the graph is a one-hot vector of size n : $\mathbf{q} = [0, 0, \dots, 1, 0, \dots]$, where $\mathbf{q}^k = 1$ and $\mathbf{q}^j = 0$ for $j = 1, \dots, n$, $j \neq k$. The task index now becomes the input signal for RDMN. With the signal from the task-specific query, the attention can identify which substructure is important for a specific task to attend on.

6 Experiments and results

In this section, we demonstrate RDMN on three applications: software vulnerability detection (single query, Section 6.1), molecular activity prediction (multiple queries, Section 6.2), and chemical reaction (query about graph-graph interaction, Section 6.3).

6.1 Software vulnerability

This application asks if a piece of source code is potentially vulnerable to security risks. In particular, we consider each Java class as a piece, which consists of attribute declarations and methods. A class is then represented as a graph, where nodes are methods and edges are function calls between methods (thus, there is only one relation type). Class-level declaration is used as query, and the answer is binary indicator of vulnerability. The dataset was collected from [15], which consists of 18 Java projects. The dataset is pre-processed by removing all replicated files of different versions in the same projects. This results in 2,836 classes of which 1,020 are potentially vulnerable.

Node and query embedding is pretrained as follows. Methods and attribute declarations of Java classes are treated as sequences of code tokens and their representation is learned through language modeling using LSTM. The feature vector of each sequence is the mean of all hidden states outputted by the LSTM. After this step, each sequence is represented as a feature vector of 128 units.

For comparison, we implemented three strong classifiers: Support Vector Machine (SVM), Random Forest (RF) and Gradient Boosting Machine (GBM) running on the averaged feature vector of all methods and attribute declarations. Fig. 3 reports the performance measured by AUC and F1-score, demonstrating the competitive results by the proposed RDMN.

6.2 Molecular bioactivities

This application asks if a chemical compound acts on a given disease. Here each compound molecule is represented as a graph, where nodes are atoms and edges are bond types

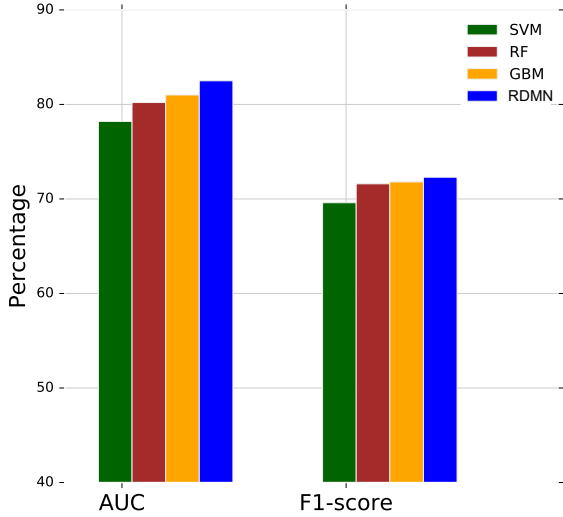


Figure 3: Performance on code vulnerability detection, measured in AUC and F1-score (%). Best viewed in color.

between them. Activity and disease form a query (e.g., coded as an one-hot vector). The answer will be binary indicator of the activity with respect to the given disease.

Datasets We conducted experiments on nine NCI **BioAssay** activity tests collected from the PubChem website⁵. Seven of them are activity tests of chemical compounds against different types of cancer: breast, colon, leukemia, lung, melanoma, central nerve system and renal. The others are AIDS antiviral assay and Yeast anticancer drug screen. Each BioAssay test contains records of activities for chemical compounds. We chose the two most common activities for classification: “active” and “inactive”. The statistics of data is reported in Table 1. The datasets are listed by the ascending order of number of active compounds. “# Graph” is the number of graphs and “# Active” is the number of active graph against a BioAssay test. These datasets are unbalanced, therefore “inactive” compounds are randomly removed so that the Yeast Anticancer dataset has 25,000 graphs and each of the other datasets has 10,000 graphs.

We used RDKit⁶ to extract the structure of molecules, the atom and the bond features. An atom feature vector is the concatenation of the one-hot vector of the atom and other features such as atom degree and number of H atoms attached. We also make use of bond features such as bond type and a binary value indicating if a bond is in a ring.

6.2.1 Experiment settings

Baselines For comparison, we use several baselines:

⁵<https://pubchem.ncbi.nlm.nih.gov/>

⁶<http://www.rdkit.org/>

Table 1: Summary of 9 NCI BioAssay datasets.

No.	Dataset	# Active	# Graph
1	AIDS Antiviral	1513	41,595
2	Renal Cancer	2,325	41,560
3	Central Nervous System	2,430	42,473
4	Breast Cancer	2,490	29,117
5	Melanoma	2,767	39,737
6	Colon Cancer	2,766	42,130
7	Lung Cancer	3,026	38,588
8	Leukemia	3,681	38,933
9	Yeast Anticancer	10,090	86,130

- *Classic classifiers running on feature vectors extracted from molecular graphs.* Classifiers are Support Vector Machine (SVM), Random Forest (RF), Gradient Boosting Machine (GBM), and multi-task neural network (MT-NN) [51]. For feature extraction, following the standard practice in the computational chemistry literature, we use the RDKit to extract molecular fingerprints – the encoding of the graph structure of the molecules by a vector of binary digits, each presents the presence or absence of particular substructures in the molecules. There are different algorithms to achieve molecular fingerprints and the state of the art is the extended-connectivity circular fingerprint (ECFP) [52]. The dimension of the fingerprint features is set by 1,024. SVM, RF and GBM predict one activity at a time, but MT-NN predict all activities at the same time.
- *Neural graphs which learn to extract features.* In particular, we use Neural Fingerprint (NeuralFP) [19]. This predicts one activity at a time.

Model setting For training neural networks, the training minimizes the cross-entropy loss in an end-to-end fashion. We use ReLU units for all steps and Dropout [59] is applied at the first and the last steps of the controller and the memory cells. We set the number of hops to $T = 10$ and other hyper-parameters are tuned on the validation dataset.

6.2.2 Results

The impact of joint training We have options to train each task separately (query set to unity, one memory per task) or to train jointly (query is an one-hot vector, shared memory for all tasks). To investigate more on how multi-task learning impacts the performance of each task, we reports the F1-score of RDMN in both separate and joint training settings on each of the nine datasets (Fig. 4). Joint training with RDMN model improves the performance of seven datasets on different types of cancers by 10%-20% on each task. However, it has little effect on AIDS antiviral and Yeast anticancer datasets. These could be explained by the fact that cancers share similar genomic footprints and thus each cancer can borrow the strength of statistics of the cancer family. This does not hold for the other conditions, which are very different from the rest. However, joint training is still desirable because we need to maintain just one model for all queries.

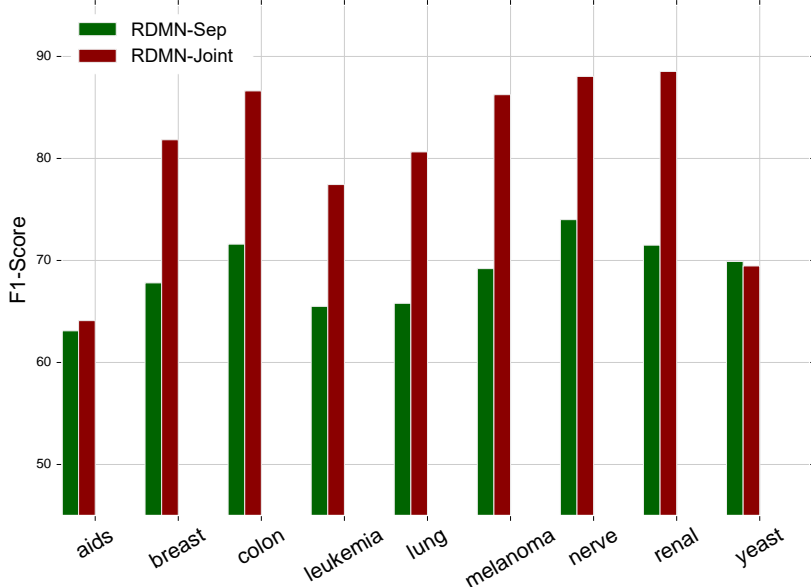


Figure 4: The comparison in performance of RDMN when training separately (RDMN-Sep) and jointly (RDMN-Joint) for all datasets. Best viewed in color.

The impact of more tasks We evaluate how the performance of RDMN on a particular dataset is affected by the number of tasks. We chose AIDS antiviral, Breast Cancer and Colon Cancer as the experimental datasets. For each experimental dataset, we start to train it and then repeatedly add a new task and retrain the model. The orders of the first three new tasks are: (AIDS, Breast, Colon) for AIDS antiviral dataset, (Breast, AIDS, Colon) for Breast Cancer dataset and (Colon, AIDS, Breast) for Colon Cancer dataset. The orders of the remaining tasks are the same for three datasets: (Leukemia, Lung, Melanoma, Nerve, Renal and Yeast).

Fig. 5 illustrates the performance of the three chosen datasets with different number of jointly training tasks. The performance of Breast and Colon Cancer datasets decreases when jointly trained with AIDS antiviral task, increases after adding more tasks, and then remains steady or slightly reduces after seven tasks. Joint training does not improve the performance on the AIDS antiviral dataset.

Comparative results Table 2 reports results, measured in Micro F1-score, Macro F1-score and the average AUC over all datasets. The best method for separated training on fingerprint features is SVM with 66.4% of Micro F1-score and on graph structure is RDMN with the improvement of 2.7% over the non-structured classifiers. The joint learning settings improve by 9.1% of Micro F1-score and 10.7 % of Macro F1-score gain on fingerprint features and 8.7% of Micro F1-score and 11.6% of Macro F1-score gain on graph structure.

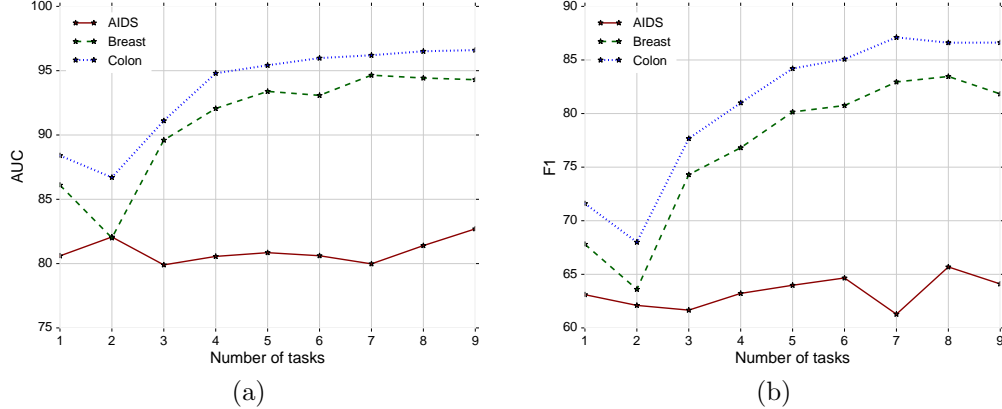


Figure 5: The performance of three datasets when increasing the number of jointly training tasks, reported in (a) AUC and (b) F1-score.

Table 2: Performance over all datasets, measured in Micro F1, Macro F1 and the average AUC.

Model	MicroF1	MacroF1	Average AUC
SVM	66.4	67.9	85.1
RF	65.6	66.4	84.7
GB	65.8	66.9	83.7
NeuralFP [19]	68.2	67.6	85.9
MT-NN [51]	75.5	78.6	90.4
RDMN	77.8	80.3	92.1

6.3 Chemical reaction

For this application we ask if two or more molecules participate in a chemical reaction. Here the queries can be whether a reaction occurs, reaction yield, or the products of a reaction given environmental conditions (e.g., temperature, pressure, catalysts). Here we limit ourselves to the first query, that is, to predict whether a reaction occurs in normal conditions. The problem can be formally formulated as prediction of graph-graph interaction, where each molecule is a graph.

Datasets We conducted experiments on chemical-chemical interaction data downloaded from the STITCH database [36] (Search Tool for InTeractions of CHemicals), a network of nearly 1M chemical interactions for over 68K different chemicals. Each interaction between two chemicals has confidence score from 0 to 999. Following [38], we extracted *positive-900* (11,764 examples) and *positive-800* (92,998) from interactions with confidence scores more than 900 and 800, respectively and extract *negative-0* (425,482 samples) from interactions with confidence scores equal to zero. We then created the CCI900 dataset from all the positive samples in positive-900 and the same number of negative samples randomly drawn from negative-0. CCI800 was also created similarly. Therefore, two datasets used for the experiments - CCI900 and CCI800 have 23,528 and 185,990 samples,

respectively. The molecules were downloaded from the PubChem database using CID (Compound ID) shown in STITCH. RDKit was used to extract graph structures, atom and bond features, fingerprints and SMILES of the molecules.

6.3.1 Experiment settings

We designed experiments on three different types of representations of molecules: (i) fingerprint features, which is described in Subsection 6.2, (ii) SMILES (Simplified Molecular-Input Line-Entry System) - a string format to describe the structures of molecules, and (iii) the graph structure information of the molecules. All these representations are extracted from molecules using the RDKit toolkit⁷.

Baselines Fingerprint feature vectors are processed by Random Forests and Highway Networks, which are two strong classifiers in many applications. Each data point consists of two fingerprint vectors representing two molecules. We average the two vectors as the input vector for the two baselines. SMILES strings are modeled by DeepCCI [38], a recent deep neural network model for chemical reactions. Each SMILES is represented by a matrix where each row is a one-hot vector of a character. The matrix is then passed through a convolution layer to learn the hidden representation for each SMILE string. The two hidden vectors are then summed and passed through a deep feedforward net to learn the final representation of the interaction between the two molecules. We tune the hyper-parameters for DeepCCI as suggested by the authors [38].

Model setting For our model, we use ReLU units for all steps and Dropout [59] is applied at the first and the last steps of the controller and the memory cells. We conducted experiments with a different number of attention heads to visualize the effect of multiple attentions. Other hyper-parameters are tuned to maximize the performance on the validation dataset.

We also conducted two other experiments to examine the effectiveness of *using side information as the query*. The attention read, which is a weighted sum of all memory cells at the controller, might not properly capture the global information of the graph while fingerprint feature vectors or SMILES strings attain this information. Here, we set two types of vectors as the queries: (i) the mean of two fingerprint vectors and (ii) the hidden representation generated by DeepCCI. For the latter setting, DeepCCI parameters are randomly initialized and jointly learned with our model’s parameters.

6.3.2 Results

The effect of multiple attentions We suppose that graph interaction is not only between the whole graphs themselves but also between the substructures from the graphs. For example, in chemical reaction, substructures from different molecules interact to create new molecules, leading to multiple substructure interactions. In our model, we expect that each attention reading head is able to capture a specific interaction of substructures. Hence, an appropriate number of attention heads can capture all substructure interactions and provide more abundant information about the graph interaction, which may improve the prediction performance. Here, we evaluated the improvement in prediction brought by

⁷<http://www.rdkit.org/>

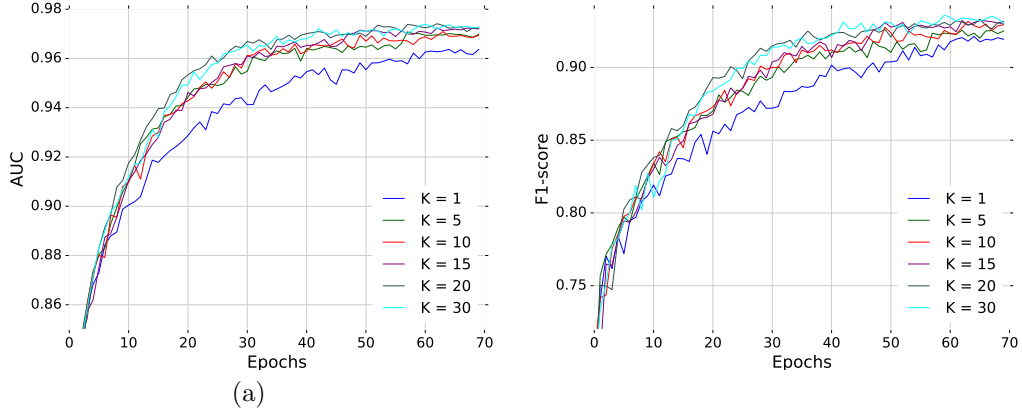


Figure 6: The performance of RDMN with different number of reading heads K during training, reported in (a) AUC and (b) F1-score. Best viewed in color.

the number of attention heads K . Taking RDMN without the side information query, we varied K by 1, 5, 10, 15, 20 and 30, and trained the resulting six models independently on CCI900 dataset. Fig. 6 reports the performance changes during training for different K . We can see that when $K > 1$, increasing K only slightly improves the performance while there is a bigger gap between the performance of $K = 1$ and $K > 1$. There is not much difference when K is increased from 20 to 30. It is possible that when the number of attention heads is large, they collect similar information from the graphs, leading to a saturation in performance.

The effect of the side information as a query While the neighborhood aggregation operation in our model can effectively capture the substructure information, the weighted sum of all memory cells in the attention mechanism might not properly collect the global information of the whole graph. Hence, using the side information containing the global information such as Fingerprints or SMILES strings might help the training. We have shown in Table 3 that using fingerprint vectors or the hidden state generated by DeepCCI as the query for our model can improve the performance on the both datasets. We also found that even using side information query increases the number of training parameters, it can prevent overfitting. Fig. 7 shows the loss curves on the training and the validation set of RDMN with a single attention head when the query is set as constant and when the query is the hidden stated produced by DeepCCI model (RDMN+SMILES). We can see from the figure that the validation loss of RDMN starts to rise quickly after 40 epochs while the validation loss of RDMN+SMILES still remains after 100 epochs.

Comparative results Table 3 reports the performance of the baselines and our proposed model in different settings on the two dataset CCI900 and CCI800 reported in AUC and F1-score. SMILES features with DeepCCI outperformed the fingerprint features with Highway Networks by 3.8% F1-score on CCI900 and by 3.6% F1-score on CCI800. Our model with a single attention head is slightly better than DeepCCI on both datasets. Interestingly, using multiple attention heads and side information (fingerprint and SMILES

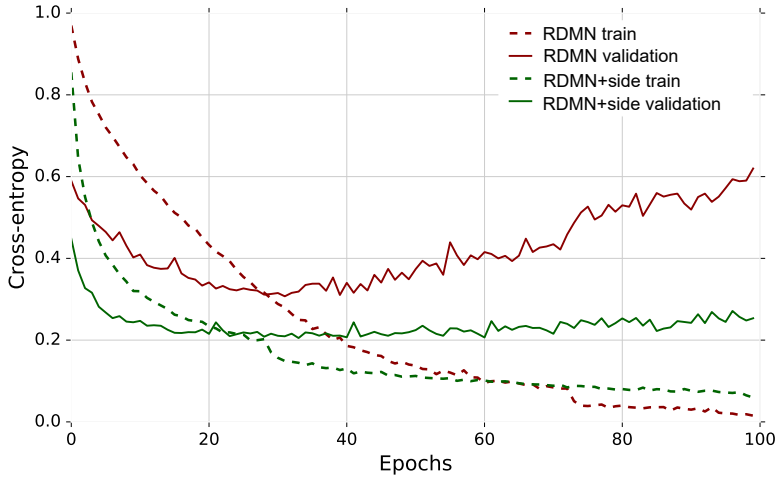


Figure 7: Training and validation losses of RDMN with and without side information during training. Best viewed in color.

features) as the query both help to improve the performance. For CCI900, RDMN with SMILES query improves 1.7% F1-score on single attention setting and 1.2% on multiple attention settings.

	CCI900		CCI800	
	AUC	F1-score	AUC	F1-score
Random Forests	94.3	86.4	98.2	94.1
Highway Networks	94.7	88.4	98.5	94.7
DeepCCI [38]	96.5	92.2	99.1	97.3
RDMN	96.6	92.6	99.1	97.4
RDMN+multiAtt	97.3	93.4	99.1	97.8
RDMN+FP	97.8	93.3	99.4	98.0
RDMN+multiAtt+FP	98.0	94.1	99.5	98.1
RDMN+SMILES	98.1	94.3	99.7	97.8
RDMN+multiAtt+SMILES	98.1	94.6	99.8	98.3

Table 3: The performance on the chemical reaction datasets reported in AUC and F1-score. *FP* stands for fingerprint and *multiAtt* stands for multiple attentions.

7 Discussion

The problem studied in this paper belongs to a broader program known as *machine reasoning*, which is defined by Leon Bottou as “algebraically manipulating previously acquired knowledge in order to answer a new question” [8]. Unlike classical focus on symbolic reasoning, here we aim for a *learnable neural reasoning* capability (e.g., see [31]).

We wish to emphasize that RDMN is a general model for answering any query about graph data. While the evaluation in this paper is limited to function calls graph, molecular bioactivity and chemical reaction, RDMN has a wide range of potential applications. For example, a drug (query) may act on the network of proteins as a whole (relational memory). In recommender systems, user can be modeled as a multi-relational graph (e.g., network between purchased items, and network of personal contacts); and query can be anything about them (e.g., preferred attributes or products). Similarly in healthcare, patient medical record can be modeled as multi-relational graphs about diseases, treatments, familial and social contexts; and query can be anything about the presence and the future of health conditions and treatments. Examples of graph-graph interaction include predicting outcome of a sport match (query), where a match can be modeled as an interaction between two team graphs (multi-memory) – here each team is a network of team members whose links are defined by their positions and the specific tactic for the match. Another application is in image-text matching (query) with image represented as *graph of objects* and text as *graph of concepts* (memory components). Finally, RDMN also generalizes set-set interactions [26], since a set is a graph without explicit links (but with implicit full connectivity).

The major limitation of the current formulation is that the memory structure in RDMN, once constructed from data graphs, is then fixed even though the content of the memory changes during the reasoning process. A future work would be deriving dynamic memory graphs that evolve with time, e.g., using the technique introduced in [67], or a gated message passing between memory cells. Also, multiple controllers may be utilized to handle asynchronous issues (e.g., see [40]) as they can partially share some memory components. Hierarchical controllers are also possible in complex settings, where low-level controllers report to a higher-level controller. This may offer a chance to implement the “meta-reasoning” faculty, where a manifestation could be selecting the right controller for a task at hand.

Conclusion

To summarize, we have proposed RDMN, a new neural network augmented with a dynamic and network-structured memory, inspired by the cognitive concept of “working memory”. We applied RDMN for three tasks: software source code vulnerability, molecular bioactivity and chemical reaction. The results are promising, demonstrating a possibility to implement trainable neural reasoning for highly complex tasks.

References

- [1] Somak Aditya, Yezhou Yang, Chitta Baral, Yiannis Aloimonos, and Cornelia Fermüller. Image understanding using vision and reasoning through scene description graph. *Computer Vision and Image Understanding*, 2017.
- [2] Miltiadis Allamanis, Marc Brockschmidt, and Mahmoud Khademi. Learning to represent programs with graphs. *ICLR*, 2018.
- [3] James Atwood and Don Towsley. Diffusion-convolutional neural networks. In *Advances in Neural Information Processing Systems*, pages 1993–2001, 2016.

- [4] Alan Baddeley. Working memory. *Science*, 255(5044):556–559, 1992.
- [5] Dzmitry Bahdanau, Kyunghyun Cho, and Yoshua Bengio. Neural machine translation by jointly learning to align and translate. *arXiv preprint arXiv:1409.0473*, 2014.
- [6] Trapit Bansal, Arvind Neelakantan, and Andrew McCallum. RelNet: End-to-end Modeling of Entities & Relations. *arXiv preprint arXiv:1706.07179*, 2017.
- [7] Min Bao, Zhi-Hao Li, and Da-Ren Zhang. Binding facilitates attention switching within working memory. *Journal of Experimental Psychology: Learning, Memory, and Cognition*, 33(5):959, 2007.
- [8] Léon Bottou. From machine learning to machine reasoning. *Machine Learning*, 94(2):133–149, 2014.
- [9] Urs Braun, Axel Schäfer, Henrik Walter, Susanne Erk, Nina Romanczuk-Seiferth, Leila Haddad, Janina I Schweiger, Oliver Grimm, Andreas Heinz, Heike Tost, et al. Dynamic reconfiguration of frontal brain networks during executive cognition in humans. *Proceedings of the National Academy of Sciences*, 112(37):11678–11683, 2015.
- [10] Michael M Bronstein, Joan Bruna, Yann LeCun, Arthur Szlam, and Pierre Vandergheynst. Geometric deep learning: going beyond euclidean data. *arXiv preprint arXiv:1611.08097*, 2016.
- [11] Joan Bruna, W Zaremba, A Szlam, and Yann LeCun. Spectral networks and deep locally connected networks on graphs. In *ICLR*, 2014.
- [12] Min-je Choi, Sehun Jeong, Hakjoo Oh, and Jaegul Choo. End-to-end prediction of buffer overruns from raw source code via neural memory networks. *IJCAI*, 2017.
- [13] George E Dahl, Navdeep Jaitly, and Ruslan Salakhutdinov. Multi-task neural networks for qsar predictions. *arXiv preprint arXiv:1406.1231*, 2014.
- [14] Hoa Khanh Dam, Trang Pham, Shien Wee Ng, Truyen Tran, John Grundy, Aditya Ghose, Taeksu Kim, and Chul-Joo Kim. A deep tree-based model for software defect prediction. *arXiv preprint arXiv:1802.00921*, 2018.
- [15] Hoa Khanh Dam, Truyen Tran, Trang Pham, Shien Wee Ng, John Grundy, and Aditya Ghose. Automatic feature learning for vulnerability prediction. *arXiv preprint arXiv:1708.02368*, 2017.
- [16] Adele Diamond. Executive functions. *Annual review of psychology*, 64:135–168, 2013.
- [17] Kien Do, Truyen Tran, Thin Nguyen, and Svetha Venkatesh. Attentional multilabel learning over graphs: A message passing approach. *arXiv preprint arXiv:1804.00293*, 2018.
- [18] Kien Do, Truyen Tran, and Svetha Venkatesh. Learning deep matrix representations. *arXiv preprint arXiv:1703.01454*, 2018.

- [19] David K Duvenaud, Dougal Maclaurin, Jorge Iparraguirre, Rafael Bombarell, Timothy Hirzel, Alán Aspuru-Guzik, and Ryan P Adams. Convolutional networks on graphs for learning molecular fingerprints. In *Advances in neural information processing systems*, pages 2224–2232, 2015.
- [20] Johan Eriksson, Edward K Vogel, Anders Lansner, Fredrik Bergström, and Lars Nyberg. Neurocognitive architecture of working memory. *Neuron*, 88(1):33–46, 2015.
- [21] David Fooshee, Aaron Mood, Eugene Gutman, Mohammadamin Tavakoli, Gregor Urban, Frances Liu, Nancy Huynh, David Van Vranken, and Pierre Baldi. Deep learning for chemical reaction prediction. *Molecular Systems Design & Engineering*, 2018.
- [22] Justin Gilmer, Samuel S Schoenholz, Patrick F Riley, Oriol Vinyals, and George E Dahl. Neural message passing for quantum chemistry. *ICML*, 2017.
- [23] Alex Graves, Greg Wayne, and Ivo Danihelka. Neural turing machines. *arXiv preprint arXiv:1410.5401*, 2014.
- [24] Alex Graves, Greg Wayne, Malcolm Reynolds, Tim Harley, Ivo Danihelka, Agnieszka Grabska-Barwińska, Sergio Gómez Colmenarejo, Edward Grefenstette, Tiago Ramalho, John Agapiou, et al. Hybrid computing using a neural network with dynamic external memory. *Nature*, 538(7626):471–476, 2016.
- [25] Klaus Greff, Rupesh K Srivastava, and Jürgen Schmidhuber. Highway and residual networks learn unrolled iterative estimation. *ICLR*, 2017.
- [26] Jason Hartford, Devon R Graham, Kevin Leyton-Brown, and Siamak Ravanbakhsh. Deep models of interactions across sets. *arXiv preprint arXiv:1803.02879*, 2018.
- [27] Kaiming He, Xiangyu Zhang, Shaoqing Ren, and Jian Sun. Deep residual learning for image recognition. *CVPR*, 2016.
- [28] Mikael Henaff, Joan Bruna, and Yann LeCun. Deep convolutional networks on graph-structured data. *arXiv preprint arXiv:1506.05163*, 2015.
- [29] Mikael Henaff, Jason Weston, Arthur Szlam, Antoine Bordes, and Yann LeCun. Tracking the world state with recurrent entity networks. *ICLR*, 2017.
- [30] Drew A Hudson and Christopher D Manning. Compositional attention networks for machine reasoning. *ICLR*, 2018.
- [31] Herbert Jaeger. Artificial intelligence: Deep neural reasoning. *Nature*, 538(7626):467, 2016.
- [32] Wengong Jin, Connor Coley, Regina Barzilay, and Tommi Jaakkola. Predicting Organic Reaction Outcomes with Weisfeiler-Lehman Network. In *Advances in Neural Information Processing Systems*, pages 2604–2613, 2017.
- [33] Daniel D Johnson. Learning graphical state transitions. *ICLR*, 2017.
- [34] Lukasz Kaiser, Ofir Nachum, Aurko Roy, and Samy Bengio. Learning to remember rare events. *ICLR*, 2017.

- [35] Thomas N Kipf and Max Welling. Semi-supervised classification with graph convolutional networks. *ICLR*, 2017.
- [36] Michael Kuhn, Christian von Mering, Monica Campillos, Lars Juhl Jensen, and Peer Bork. Stitch: interaction networks of chemicals and proteins. *Nucleic acids research*, 36(suppl_1):D684–D688, 2007.
- [37] Ankit Kumar, Ozan Irsoy, Jonathan Su, James Bradbury, Robert English, Brian Pierce, Peter Ondruska, Ishaan Gulrajani, and Richard Socher. Ask me anything: Dynamic memory networks for natural language processing. *ICML*, 2016.
- [38] Sunyoung Kwon and Sungroh Yoon. DeepCCI: End-to-end Deep Learning for Chemical-Chemical Interaction Prediction. *arXiv preprint arXiv:1704.08432*, 2017.
- [39] Hung Le, Truyen Tran, Thin Nguyen, and Svetha Venkatesh. Variational memory encoder-decoder. *arXiv preprint arXiv:1807.09950*, 2018.
- [40] Hung Le, Truyen Tran, and Svetha Venkatesh. Dual memory neural computer for asynchronous two-view sequential learning. *KDD*, 2018.
- [41] Yujia Li, Daniel Tarlow, Marc Brockschmidt, and Richard Zemel. Gated graph sequence neural networks. *ICLR*, 2016.
- [42] Yujia Li, Oriol Vinyals, Chris Dyer, Razvan Pascanu, and Peter Battaglia. Learning deep generative models of graphs. *arXiv preprint arXiv:1803.03324*, 2018.
- [43] Leonid Libkin, Wim Martens, and Domagoj Vrgoč. Querying graphs with data. *Journal of the ACM (JACM)*, 63(2):14, 2016.
- [44] Gianluigi Mongillo, Omri Barak, and Misha Tsodyks. Synaptic theory of working memory. *Science*, 319(5869):1543–1546, 2008.
- [45] Mathias Niepert, Mohamed Ahmed, and Konstantin Kutzkov. Learning convolutional neural networks for graphs. In *Proceedings of the 33rd annual international conference on machine learning*. ACM, 2016.
- [46] Emilio Parisotto and Ruslan Salakhutdinov. Neural map: Structured memory for deep reinforcement learning. *ICLR*, 2018.
- [47] Ethan Perez, Florian Strub, Harm De Vries, Vincent Dumoulin, and Aaron Courville. Film: Visual reasoning with a general conditioning layer. *arXiv preprint arXiv:1709.07871*, 2017.
- [48] Trang Pham, Truyen Tran, Dinh Phung, and Svetha Venkatesh. Faster training of very deep networks via p-norm gates. *ICPR*, 2016.
- [49] Trang Pham, Truyen Tran, Dinh Phung, and Svetha Venkatesh. Column networks for collective classification. *AAAI*, 2017.
- [50] Trang Pham, Truyen Tran, and Svetha Venkatesh. Graph memory networks for molecular activity prediction. *ICPR*, 2018.

- [51] Bharath Ramsundar, Steven Kearnes, Patrick Riley, Dale Webster, David Konerding, and Vijay Pande. Massively multitask networks for drug discovery. *arXiv preprint arXiv:1502.02072*, 2015.
- [52] David Rogers and Mathew Hahn. Extended-connectivity fingerprints. *Journal of chemical information and modeling*, 50(5):742–754, 2010.
- [53] Adam Santoro, Sergey Bartunov, Matthew Botvinick, Daan Wierstra, and Timothy Lillicrap. Meta-learning with memory-augmented neural networks. In *International conference on machine learning*, pages 1842–1850, 2016.
- [54] Adam Santoro, Ryan Faulkner, David Raposo, Jack Rae, Mike Chrzanowski, Theophane Weber, Daan Wierstra, Oriol Vinyals, Razvan Pascanu, and Timothy Lillicrap. Relational recurrent neural networks. *arXiv preprint arXiv:1806.01822*, 2018.
- [55] Adam Santoro, David Raposo, David G Barrett, Mateusz Malinowski, Razvan Pascanu, Peter Battaglia, and Tim Lillicrap. A simple neural network module for relational reasoning. In *Advances in neural information processing systems*, pages 4974–4983, 2017.
- [56] Franco Scarselli, Marco Gori, Ah Chung Tsoi, Markus Hagenbuchner, and Gabriele Monfardini. The graph neural network model. *IEEE Transactions on Neural Networks*, 20(1):61–80, 2009.
- [57] Michael Schlichtkrull, Thomas N Kipf, Peter Bloem, Rianne van den Berg, Ivan Titov, and Max Welling. Modeling relational data with graph convolutional networks. *arXiv preprint arXiv:1703.06103*, 2017.
- [58] Richard Socher, Danqi Chen, Christopher D Manning, and Andrew Ng. Reasoning with neural tensor networks for knowledge base completion. In *Advances in Neural Information Processing Systems*, pages 926–934, 2013.
- [59] Nitish Srivastava, Geoffrey Hinton, Alex Krizhevsky, Ilya Sutskever, and Ruslan Salakhutdinov. Dropout: A simple way to prevent neural networks from overfitting. *Journal of Machine Learning Research*, 15:1929–1958, 2014.
- [60] Rupesh K Srivastava, Klaus Greff, and Jürgen Schmidhuber. Training very deep networks. In *Advances in neural information processing systems*, pages 2377–2385, 2015.
- [61] Mark G Stokes. ‘activity-silent’ working memory in prefrontal cortex: a dynamic coding framework. *Trends in cognitive sciences*, 19(7):394–405, 2015.
- [62] Sainbayar Sukhbaatar, Arthur Szlam, Jason Weston, and Rob Fergus. End-to-end memory networks. *NIPS*, 2015.
- [63] Thomas Unterthiner, Andreas Mayr, Günter Klambauer, and Sepp Hochreiter. Toxicity prediction using deep learning. *arXiv preprint arXiv:1503.01445*, 2015.
- [64] S Vichy N Vishwanathan, Nicol N Schraudolph, Risi Kondor, and Karsten M Borgwardt. Graph kernels. *Journal of Machine Learning Research*, 11(Apr):1201–1242, 2010.

- [65] Ronald J Williams. Simple statistical gradient-following algorithms for connectionist reinforcement learning. *Machine learning*, 8(3-4):229–256, 1992.
- [66] Caiming Xiong, Victor Zhong, and Richard Socher. Dynamic coattention networks for question answering. *ICLR*, 2017.
- [67] Rex Ying, Jiaxuan You, Christopher Morris, Xiang Ren, William L Hamilton, and Jure Leskovec. Hierarchical graph representation learning withdifferentiable pooling. *arXiv preprint arXiv:1806.08804*, 2018.
- [68] Jiaxuan You, Rex Ying, Xiang Ren, William L Hamilton, and Jure Leskovec. GraphRNN: A Deep Generative Model for Graphs. *arXiv preprint arXiv:1802.08773*, 2018.